

An Isocyanide Probe for Heme Electronic Structure: **Bis(*tert*-butylisocyanide) Complex of Diazaporphyrin Showing a Unique $(d_{xy})^2(d_{xz}, d_{yz})^3$ Ground State**

Yoshiki Ohgo,^{a,b,*} Saburo Neya,^c Hidehiro Uekusa,^d and Mikio Nakamura^{a,b,e,*}

^aDepartment of Chemistry, School of Medicine, Toho University, Ota-ku, Tokyo 143-8540, Japan, ^bResearch Center for Materials with Integrated Properties, Toho University, Funabashi, 274-8510, Japan, ^cDepartment of Physical Chemistry, Graduate school of Pharmaceutical Sciences, Chiba University, Chiba 263-8522, Japan, ^dDepartment of Chemistry and Materials Science, Tokyo Institute of Technology, Tokyo 152-8551, Japan, ^eDivision of Chemistry, Graduate School of Science, Toho University, Funabashi, Chiba 274-8510, Japan.

Supplementary Information

1) Experimental

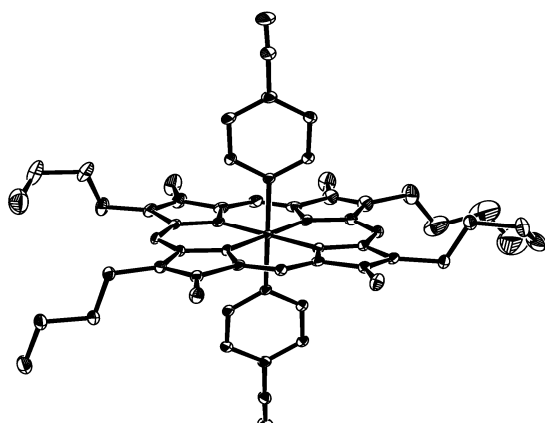
$H_2(DAzP)$ was prepared by the literature methods.^{*} $H_2(OEP)$ was purchased from Aldrich. Insertion of iron with $FeCl_2 \cdot 4H_2O$ followed by the HCl treatment afforded the corresponding chlorides, $Fe(DAzP)Cl$ and $Fe(OEP)Cl$. These chlorides were converted to the perchlorates, $Fe(DAzP)ClO_4$ and $Fe(OEP)ClO_4$, by the addition of THF solution of $AgClO_4$, which were further converted to the corresponding six-coordinated complexes, $[Fe(Por)L_2]^+(1-4)$, by the addition of 5-10 equiv of the ligand ($L = {}^tBuNC$ or DMAP or 4-CNPy). Corresponding low-spin Co(III) complexes, $[Co(Por)L_2]^+$, were synthesized by same way as described above, and were used as diamagnetic references in the spin density analysis. The solid samples were purified by recrystallization from dichloromethane. Although structural analysis of $[Fe(DAzP)({}^tBuNC)_2]^+$ is unsuccessful at this point, we were able to determine the molecular structure of analogous $[Fe(DAzP)(4-CNPy)_2]^+$. The geometric factors of the protons and carbons in **1** and **2** were estimated on the basis of the structural parameters of $[Fe(DAzP)(4-CNPy)_2]^+$. All data set for this complex were collected at 80K on a Rigaku RAXIS-RAPID Imaging Plate diffractometer with $MoK\alpha$ radiation ($\lambda=0.71073\text{\AA}$). Crystallographic data was deposited to the Cambridge Crystallographic Data Centre (CCDC) as supplementary publication no. CCDC-606379. Copies of the data can be obtained free of charge on application to CCDC, 12 Union Road, Cambridge CB21EZ, UK (fax: (+44) 1233-336-033; e-mail: deposit@ccdc.cam.ac.uk). 1H and ^{13}C NMR spectra were recorded on a JEOL LA300 spectrometer operating at 300.4 MHz for proton. EPR spectra were measured at 12K with a Bruker E500 spectrometer operating at X band and equipped with an Oxford helium cryostat. IR spectra were measured with SHIMAZU FTIR-8100.

^{*}O. G. Khelevina, N. V. Chizhova, P. A. Stuzhin, A. S. Semeikin, B. D. Berezin, Russ. J. Phys. Chem. (Engl. Transl) 1997, 71, 74-78.

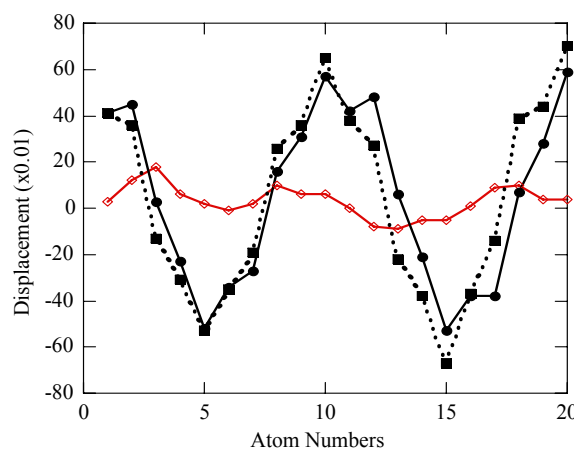
2) Molecular structure of $[\text{Fe}(\text{DAzP})(4\text{-CNPY})_2]\text{ClO}_4$.

Figure S1(a) shows the molecular structure of analogous $[\text{Fe}(\text{DAzP})(4\text{-CNPY})_2]^+$ determined by X-ray crystallography. The average bond length between iron and pyrrole nitrogens (Fe-N_p) and that between iron and axial ligands (Fe-N_{ax}) were $1.948(3)$ Å and $2.032(3)$ Å, respectively. Thus, $[\text{Fe}(\text{DAzP})(4\text{-CNPY})_2]^+$ has extremely short Fe-N_p bonds as compared with low-spin 6-coordinate iron(III) porphyrinates with planar porphyrin core such as $[\text{Fe(OEP)}(\text{DMAP})_2]\text{ClO}_4$; $\text{Fe-N}_p = 2.00$ Å.

All the peripheral carbon and nitrogen atoms are located nearly on the mean macrocycle plane as shown in Figure S1(b); the maximum deviation of these atoms was less than 0.20 Å. For comparison, the core conformations of $[\text{Fe}(\text{TPP})(4\text{-CNPY})_2]\text{ClO}_4$ and $[\text{Fe}(\text{TPP})(^{\prime}\text{BuNC})_2]\text{ClO}_4$ are also given in Figure S1(b).



(a)



(b)

Figure S1. (a) Molecular structure of $[\text{Fe}(\text{DAzP})(4\text{-CNPY})_2]\text{ClO}_4$. The ellipsoids are drawn at 50% probability. (b) Perpendicular displacements of the peripheral 20 carbon atoms from the least-squares plane of the macrocycles.; \diamond : $[\text{Fe}(\text{DAzP})(^{\prime}\text{BuNC})_2]\text{ClO}_4$, \bullet : $[\text{Fe}(\text{TPP})(4\text{-CNPY})_2]\text{ClO}_4$, \blacksquare : $[\text{Fe}(\text{TPP})(^{\prime}\text{BuNC})_2]\text{ClO}_4$.

3) Validity of using geometric factors obtained from the molecular structure of analogous

[Fe(DAzP)(4-CNPy)₂]ClO₄:

As described in the manuscript, the geometric factors for the spin density analysis in [Fe(DAzP)(^tBuNC)₂]ClO₄ (**1**) and [Fe(DAzP)(^tBuNC)₂]ClO₄ (**2**) were estimated from the X-ray structural data of analogous [Fe(DAzP)(4-CNPy)₂]ClO₄. As shown in Figure S1(b), [Fe(DAzP)(4-CNPy)₂]ClO₄ has a quite planar DAzP core. In contrast, [Fe(TPP)(4-CNPy)₂]ClO₄ and [Fe(TPP)(^tBuNC)₂]ClO₄ exhibit highly ruffled porphyrin cores because of the (d_{xz}, d_{yz})⁴(d_{xy})¹ ground state. The degree of ruffling in [Fe(TPP)(4-CNPy)₂]ClO₄ is quite close to that in [Fe(TPP)(^tBuNC)₂]ClO₄. Furthermore, the average bond distances between iron and pyrrole nitrogen atoms in [Fe(TPP)(4-CNPy)₂]⁺ and [Fe(TPP)(^tBuNC)₂]⁺ are both 1.95 Å. Thus, the structural parameters of these two complexes are almost identical. We have then considered that the geometric factors of the protons and carbon atoms in [Fe(DAzP)(4-CNPy)₂]⁺ should also be quite close to those in [Fe(DAzP)(^tBuNC)₂]⁺ (**1**) and [Fe(DAzP)(DMAP)₂]⁺ (**2**) since all of these complexes adopt the (d_{xy})²(d_{xz}, d_{yz})³ ground state. We have estimated the dipolar shifts of the proton and carbon signals of **1** and **2** by using the geometric factors of [Fe(DAzP)(4-CNPy)₂]⁺, and then determined the contacts shifts, from which the spin densities have been calculated as given in Table 1 of the manuscript. As for the detailed procedure to obtain spin densities, see ref. 6.

4) ^1H NMR, ^{13}C NMR, and EPR Data.

Table S1. ^1H NMR Chemical Shifts(CD_2Cl_2 , 298 K, δ ppm)

Complexes	meso	CH_3	$\text{CH}_2(\alpha)$	$\text{CH}_2(\beta)$	<i>tert</i> -C(CH ₃) ₃
1	19.20	35.2	17.9	2.3	3.6 ^{a)}
2	3.52	20.2	7.2	-1.0	—
3	-37.7	7.6(α)	3.2(β)	-0.8	—
4	1.8	6.7(α)	-0.4(β)	—	—
[Co(DAzP)(^t BuNC) ₂] ⁺	10.17	3.70	4.11	2.27	-0.68
[Co(DAzP)(DMAP) ₂] ⁺	10.19	3.61	4.04	2.32	—
[Co(OEP)(^t BuNC) ₂] ⁺	10.04	4.05(α)	1.80(β)	-0.91	—
[Co(OEP)(DMAP) ₂] ⁺	10.07	4.10(α)	1.96(β)	—	—

a) broad.

Table S2. ^{13}C NMR Chemical Shifts(CD_2Cl_2 , 298 K, δ ppm)

Complexes	meso	α	β	$\text{CH}_3(\alpha)$	$\text{CH}_2(\alpha)$	$\text{CH}_2(\beta)$
1	33.5	68.5, 25.2	181.6, 185.3	-59.3	-35.2	129.7
2	6.9	32.0, 35.9	161.9, 147.1	-45.8	-21.8	91.0
3	371.4	-94.9(α)	115.9(β)	1.7(α)	54.0(β)	—
4	21.9	51.9(α)	157.9(β)	-23.5(α)	80.9(β)	—
[Co(DAzP)(^t BuNC) ₂] ⁺	99.5	142.4, 147.5	147.2, 142.4	11.8	26.7	35.1
[Co(DAzP)(DMAP) ₂] ⁺	100.0	143.0, 148.5	141.0, 145.6	11.7	26.9	35.4
[Co(OEP)(^t BuNC) ₂] ⁺	96.3	146.9(α)	140.8(β)	20.4(α)	18.9(β)	—
[Co(OEP)(DMAP) ₂] ⁺	96.7	144.9(α)	141.0(β)	20.4(α)	18.3(β)	—

Table S3. EPR g Values(CH_2Cl_2 , 4-12 K)

Complexes	g_1	g_2	g_3
1	3.01	2.05	1.5
2	2.82	2.22	1.62
3	2.29	2.29	1.86
4	2.82	2.28	1.64